PHYSICAL REVIEW D **96,** 114001 (2017)

Color entanglement like effect in collinear twist-3 factorization

Jian Zhou

School of Physics and Key Laboratory of Particle Physics and Particle Irradiation (MOE), Shandong University, Jinan, Shandong 250100, China

(Received 21 July 2017; published 1 December 2017)

We study the color entanglement like effect for T-odd cases in collinear twist-3 factorization. For an example, we compute the transverse single spin asymmetry for direct photon production in pp collisions in a pure collinear twist-3 approach. By analyzing the gauge link structure of the collinear gluon distribution on the unpolarized target side, we demonstrate how the color entanglement–like effect arises in the presence of the additional gluon attachment from a polarized projectile. The result is consistent with that obtained from a hybrid approach calculation.

DOI: 10.1103/PhysRevD.96.114001

I. INTRODUCTION

One of the key steps involved in proving QCD factorization theorems is to decouple longitudinal gluon exchange between active partons and the remnants of projectile/target nucleons in a high-energy scattering process. By invoking the Ward identity argument, longitudinal gluon exchange to all orders can be absorbed into a gauge link that ensures the gauge invariance of the operator definitions of parton distribution functions. In the context of the transverse momentum–dependent (TMD) factorization framework [1], depending on color flow in a hard scattering, TMD parton distributions could possess a quite complicated gauge link structure [2–5]. A generalized TMD factorization was proposed [3,4] to express cross sections in terms of process-dependent TMDs when computing physical observables that are sensitive to incoming parton transverse momenta.

However, further investigation [6] reveals that it is not possible to disentangle simultaneous longitudinal gluon attachments from both nucleon sides in nucleon-nucleon collisions if color flow is nontrivial in the final state. This phenomenon, commonly refereed to as color entanglement, originates from the non-Abelian feature of QCD as a gauge theory. It prevents us from describing parton transverse momentum with separate correlation functions for each external nucleon and thus leads to the breakdown of generalized TMD factorization. The phenomenological implications of the color entanglement like effect have been explored from both theoretical and experimental sides [7–10].

On the other hand, it is not yet entirely clear whether a similar effect shows up in nucleon-nucleon collisions in collinear factorization calculation. Though it is usually believed to be absent in leading-twist collinear factorization, at twist-3 level, one has to take into account an additional gluon rescattering, which makes color flow more complicated and could potentially give rise to the color entanglement–like effect. In fact, the transverse single spin asymmetry (SSA) for prompt photon production in pp collisions computed in genuine collinear twist-3 factorization [11,12] differs from that obtained in the hybrid approach [13] by terms proportional to a new gluon distribution G_4. This new contribution results from the color entanglement–like effect, which describes the emergence of the nontrivial color structure when taking into account longitudinal gluon attachments from both incoming nucleons. In contrast to the color entanglement like effect in the context of TMD factorization, the color entanglement–like effect does not lead to factorization breaking in the hybrid approach and the collinear factorization as shown below.

To some extent, the hybrid approach is a more complete method in the sense that gluon rescattering on the unpolarized target side has been summed to all orders. One thus has good reason to believe that the color entanglement–like effect related to the G_4 term contribution is missing in the conventional collinear twist-3 calculation. The objective of this paper is to explicitly work out color structure for the diagrams with simultaneous longitudinal gluon attachments from both incoming nucleon sides within the pure collinear twist-3 factorization framework. To the best of our knowledge, the gauge link structure of leading-twist collinear parton distributions on the unpolarized target side has never been carefully examined in the presence of an additional gluon attachment from a polarized projectile. To identify the color entanglement–like effect and compare it with the hybrid approach, it is sufficient to take into account one longitudinal gluon attachment from the unpolarized target on each side of the cut, since this is the lowest nontrivial order at which G_4 receives a nonvanishing contribution. As discussed in Sec. III, the gluon distribution G_4 indeed enters into the spin-dependent cross section in a pure collinear twist-3 approach when going beyond one gluon exchange approximation. As expected, we verified that the hybrid approach and the collinear twist-3 approach yield the same result in the collinear limit at the order under consideration.

The paper is structured as follows. In the next section, we briefly review the conventional collinear twist-3

calculations for the SSA in direct photon production and the derivation of the gauge link of the collinear gluon distribution in leading-twist collinear factorization. In Sec. III, we present our analysis for the gauge link structure at twist-3 level in detail and recover the hybrid approach result. In the end, we comment on more general cases and discuss possible extensions of the current work in Sec. IV.

II. BRIEF REVIEW OF CONVENTIONAL CALCULATIONS

The dominant production mechanism for prompt photons in high-energy collisions is Compton scattering $gq \to \gamma q$ as shown in Fig. 1. We start by introducing the relevant kinematical variables and assign 4-momenta to the particles according to

$$g(x'\bar{P}) + q(xP) \to \gamma(l_\gamma) + q(l_q), \tag{1}$$

where $\bar{P}^\mu = \bar{P}^- n^\mu$ and $P^\mu = P^+ p^\mu$ with n^μ and p^μ being the commonly defined light cone vectors, normalized according to $p \cdot n = 1$. The corresponding unpolarized Born cross section reads

$$\frac{d^3\sigma}{d^2 l_{\gamma\perp} dz} = \frac{\alpha_s \alpha_{em}}{N_c} \frac{z[1+(1-z)^2]}{l_{\gamma\perp}^4} \sum_q e_q^2 \int_{x_{\min}}^1 dx f_q(x) x' G(x'), \tag{2}$$

where $z \equiv l_\gamma \cdot n/(xP \cdot n)$ is the fraction of the incoming quark momentum xP carried by the outgoing photon and $l_{\gamma\perp}$ is the photon transverse momentum. The meaning of the other coefficients should be self-evident. Note that $x' = \frac{xP \cdot l_q}{xP \cdot \bar{P} - P \cdot l_\gamma}$ is a function of x, and $x_{\min}$ is given by $x_{\min} = \frac{P \cdot l_\gamma}{P \cdot \bar{P} - P \cdot l_q}$. In the above formula, $f_q(x)$ and $G(x')$ are the usual integrated quark and gluon distributions, respectively.

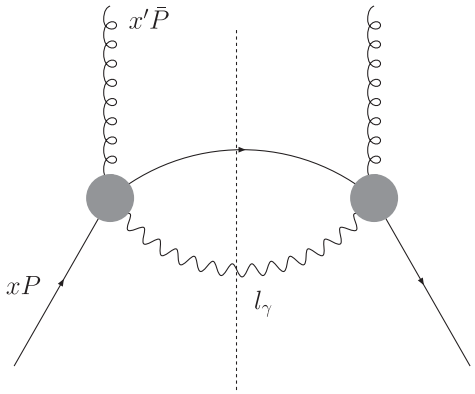

FIG. 1. Diagram contributing to direct photon production in pp collisions. Gray circles indicate all possible photon line attachments.

The operator definition of the collinear gluon distribution is given by [1]

$$x'G(x') = \int \frac{d\xi^+}{2\pi \bar{P}^-} e^{-ix'\bar{P}^-\xi^+} \langle P | F_a^{-\mu}(\xi^+) \tilde{\mathcal{L}}_{ac} F_c^{-\mu}(0) | P \rangle, \tag{3}$$

where $F_a^{-\mu}$ is the gauge field strength tensor and $\tilde{\mathcal{L}}_{ac} = \mathcal{P}\exp\{-g\int_0^{\xi^+} dz^+ f^{bac} A_b^-(z)\}$ is the gauge link in the adjoint representation. This gluon distribution can also be defined in the fundamental representation [14],

$$x'G(x') = 2\int \frac{d\xi^+}{2\pi \bar{P}^-} e^{-ix'\bar{P}^-\xi^+} \times \langle P | \mathrm{Tr}[F_a^{-\mu}(\xi^+) T^a \mathcal{L} F_c^{-\mu}(0) T^c \mathcal{L}^\dagger] | P \rangle, \tag{4}$$

where the gauge link takes form $\mathcal{L} = \mathcal{P}\exp\{-ig\int_0^{\xi^+} dz^+ T^b A_b^-(z)\}$.

The above gauge link is built up by summing longitudinal gluon (A^-) attachment to all orders. As a warm-up exercise, we first rederive the gauge link at lowest nontrivial order by computing the diagrams illustrated in Fig. 2. The gluon pole and the color structure associated with the initial-state interaction in the amplitude is given by

$$\frac{1}{x_g' + i\epsilon} \mathrm{Tr}[T^a T^c T^b], \tag{5}$$

which yields the following contribution to the first-order expansion of the gauge link:

$$\langle P | \mathrm{Tr}\left[F_a^{-\mu}(\xi^+) T^a F_c^{-\mu}(0) T^c \left(-ig \int_{-\infty}^0 dz^+ T^b A_b^-(z) \right) \right] | P \rangle. \tag{6}$$

And similarly, for the final-state interaction in the amplitude, one has

$$\frac{1}{-x_g' + i\epsilon} \mathrm{Tr}[T^a T^b T^c] \Rightarrow \langle P | \mathrm{Tr}\left[F_a^{-\mu}(\xi^+) T^a \left(-ig \int_0^\infty dz^+ T^b A_b^-(z) \right) \times F_c^{-\mu}(0) T^c \right] | P \rangle. \tag{7}$$

For Fig. 2(c), one has

$$\frac{1}{x_g' - i\epsilon} \mathrm{Tr}[T^b T^a T^c] \Rightarrow \langle P | \mathrm{Tr}\left[\left(ig \int_{-\infty}^{\xi^+} dz^+ T^b A_b^-(z) \right) \times F_a^{-\mu}(\xi^+) T^a F_c^{-\mu}(0) T^c \right] | P \rangle, \tag{8}$$

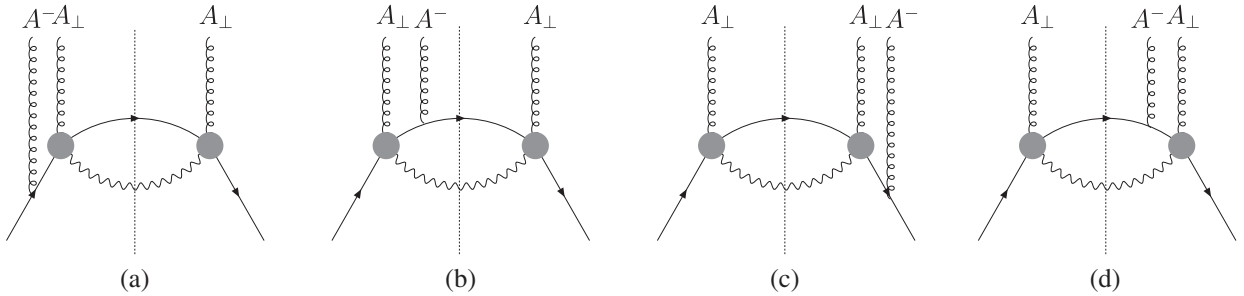

FIG. 2. The lowest-order diagrams contributing to the gauge link of the integrated gluon distribution. Both the intial state intercation shown in (a) and (c) and the final state interaction shown in (b) and (d) contribute to the gauge link.

and in Fig. 2(d),

$$\frac{1}{-x_g' - i\epsilon}\mathrm{Tr}[T^a T^b T^c] \Rightarrow \langle P|\mathrm{Tr}\left[F_a^{-\mu}(\xi^+)T^a\left(ig\int_{\xi^+}^{\infty} dz^+ T^b A_b^-(z)\right)\times F_c^{-\mu}(0)T^c\right]|P\rangle. \tag{9}$$

Summing up all terms gives rise to the first nontrivial order expansion of the gauge link. It is easy to generalize the above derivation and absorb longitudinal gluon exchange into the gauge link to all orders. Meanwhile, the gauge link of the integrated quark distribution from the projectile nucleon is built up by summing the longitudinal gluon A^+ attachment. One does not expect that these two procedures (summing A^- and A^+ gluon exchanges) interfere with each other at leading-twist level.

We now turn to review the conventional twist-3 calculation for the SSA in the prompt photon production process [11,12]. In a covariant gauge calculation, as shown in Fig. 3, an additional A^+ gluon that carries small transverse momentum $p_\perp$ must be exchanged in order to generate an imaginary phase necessary for the nonvanishing SSA. One can isolate the imaginary part by picking up gluon poles generated via the initial-state interactions or the final-state interactions as shown in Fig. 3. However, as is well known, there is a complete cancelation between the contributions from the different cut diagrams with a longitudinal gluon attaching to the unobserved final-state produced particle. This can be best seen by explicitly writing down the gluon pole contribution and the on-shell condition from Fig. 3(c),

$$\left.\frac{1}{(l_q - x_g P - k_\perp)^2 + i\epsilon}\right|_{\mathrm{pole}} \delta(l_q^2) = -i\pi\delta((l_q - x_g P - k_\perp)^2)\delta(l_q^2), \tag{10}$$

and from the left cut diagram, Fig. 3(d),

$$\left.\frac{1}{l_q^2 - i\epsilon}\right|_{\mathrm{pole}} \delta((l_q - x_g P - k_\perp)^2) = +i\pi\delta(l_q^2)\delta((l_q - x_g P - k_\perp)^2), \tag{11}$$

where $l_q = xP + x'\bar{P} + x_g P + p_\perp - l_\gamma$. Obviously, they cancel each other out as the remaining parts of the amplitude squared represented by Figs. 3(c) and 3(d) are exactly same. The absence of the final-state interaction contributions to the SSA in the current case is actually the key observation that leads us to conclude that the color entanglement like effect also shows up in collinear twist-3 factorization. We will explain the reasoning in details in the next section.

To isolate the twist-3 effect, one proceeds by expanding the amplitudes squared and the on-shell condition in terms of $p_\perp$,

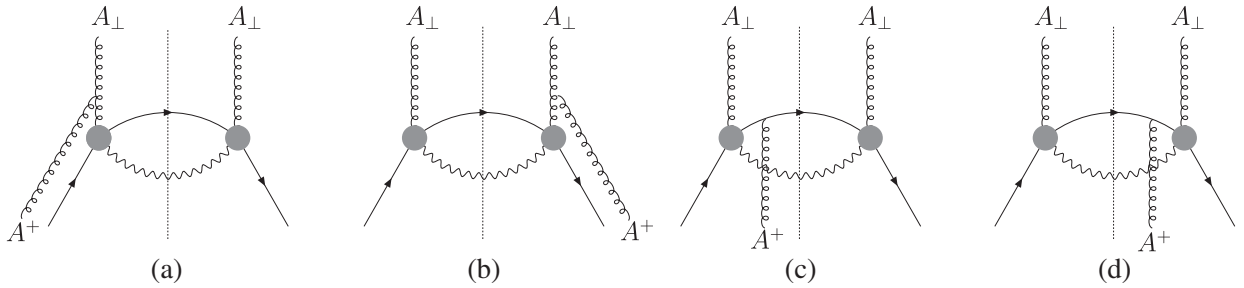

FIG. 3. Soft gluon pole contributions to the single spin asymmetry for direct photon production in pp collisions. Final-state interaction contributions (c) and (d) to the spin asymmetry cancel out. The spin asymmetry only arises from the initial state interaction shown in (a) and (b) in this process. Note that A^+ gluon carries small transverse momentum in the twist-3 calculation.

$$\mathcal{H}(p_\perp)\delta(l_q^2) = \mathcal{H}(p_\perp)\delta(l_q^2)|_{p_\perp=0} + \left.\frac{\partial \mathcal{H}(p_\perp)\delta(l_q^2)}{\partial p_\perp^\rho}\right|_{p_\perp=0} p_\perp^\rho + \cdots \quad (12)$$

The twist-3 spin-dependent part is the term linear in $p_\perp$. In this work, we only take into account the derivative term contribution, for which case our analysis can be greatly simplified without losing generality. For the derivative term contribution, one can simply neglect $p_\perp$ in the hard part $\mathcal{H}$,

$$\frac{-l_{\gamma\perp}^\rho}{l_q\cdot P}\mathcal{H}(p_\perp=0)\left[\frac{\partial\delta(l_q^2)}{\partial x}\right]_{p_\perp=0} p_{\perp,\rho}. \quad (13)$$

One then can carry out integration over $p_\perp$ after converting A^+ into the gauge-invariant form $F^{\rho+}$ by partial integration. The corresponding three-parton correlation function can be cast into the form of the Efremov-Teryaev-Qiu-Sterman (ETQS) function defined as [15,16]

$$T_{F,q}(x_1,x_2) = \int \frac{dy_1^- dy_2^-}{4\pi} e^{ix_1P^+y_1^- + i(x_2-x_1)P^+y_2^-} \times \langle P,S_\perp|\bar\psi_q(0)\gamma^+ g\epsilon^{S_\perp\rho np}F_\rho{}^+(y_2^-)\psi_q(y_1^-)|P,S_\perp\rangle, \quad (14)$$

where we have suppressed gauge links. $S_\perp$ denotes the proton transverse spin vector. Note that our definition of the ETQS functions differs by a factor g from the convention used in Ref. [12].

Making use of the ingredients described above, the calculation is straightforward. The derivative term contribution to the spin-dependent cross section is given in Refs. [11,12],

$$\frac{d^3\Delta\sigma}{d^2l_{\gamma\perp}dz} = \frac{\alpha_s\alpha_{em}N_c}{N_c^2-1}\frac{(z^2-z)[1+(1-z)^2]}{l_{\gamma\perp}^4}\frac{\epsilon^{l_\gamma S_\perp np}}{l_{\gamma\perp}^2} \times\sum_q e_q^2\int_{x_{\min}}^1 dx x'G(x')\left[-x\frac{d}{dx}T_{F,q}(x,x)\right]. \quad (15)$$

The same observable has also been computed in a hybrid approach [13]. It has been found that two approaches do not produce the same result. To be more explicit, $x'G(x')$ in the above formula is replaced with the combination $x'G(x')-x'G_4(x')$ in the hybrid approach calculation in the collinear limit. Numerically, the impact of G_4 on the SSA for photon production is limited as G_4 is $1/N_c^2$ suppressed as compared to the normal integrated gluon distribution G [13,17,18]. However, a recent work [19] shows that the SSA for the forward inclusive jet production in pp/pA collisions is proportional to the combination $x'G(x')-N_c^2x'G_4(x')$, which drastically deviates from the prediction of the conventional collinear twist-3 calculations. Therefore, from both the theoretical and phenomenological points of view, it is important to pin down the source of the inconsistency between two approaches. We address this issue in the next section.

III. GAUGE LINK STRUCTURE IN COLLINEAR TWIST-3 FACTORIZATION

The new gluon distribution G_4 appears in the hybrid approach calculation results from the color entanglement–like effect that arises when considering A^+ and A^- gluon exchanges from each side simultaneously. The operator definition of the integrated G_4 reads [17]

$$x'G_4(x') = \frac{2}{N_c}\int\frac{d\xi^+}{2\pi\bar P^-}e^{-ix'\bar P^-\xi^+} \times\langle P|\mathrm{Tr}[\mathcal{L}_\xi F^{-\mu}(\xi^+)]\mathrm{Tr}[\mathcal{L}_0^\dagger F^{-\mu}(0)]|P\rangle, \quad (16)$$

where the gauge link is given by

$$\mathcal{L}_\xi = \mathcal{P}\exp\left[ig\int_{\xi^+}^{+\infty}dz^+A^-(z^+,0_\perp)\cdot T\right] \times\mathcal{P}\exp\left[ig\int_0^{+\infty}dz_\perp A_\perp(+\infty^+,z_\perp)\cdot T\right] \times\mathcal{P}\exp\left[ig\int_{+\infty}^{0}dz_\perp A_\perp(-\infty^+,z_\perp)\cdot T\right] \times\mathcal{P}\exp\left[ig\int_{-\infty}^{\xi^+}dz^+A^-(z^+,0_\perp)\cdot T\right] \quad (17)$$

with transverse gauge links [20,21] being included. We are now aiming to recover the above novel color structure within the pure collinear twist-3 formalism. Before making an all-order analysis, it is instructive to carry out an explicit calculation at lowest nontrivial order. To this end, one has to compute diagrams with one A^- gluon attachment on each side of cut due to $\mathrm{Tr}[T^a]=0$.

As we focus on the derivative term contribution, we can neglect transverse momentum $p_\perp$ carried by the A^+ gluon in the hard parts except for $p_\perp$ dependence in the on-shell condition $\delta(l_q^2)$. The hard parts computed from different diagrams are then proportional to the twist-2 spin-independent Born diagram contribution, but with different gluon pole and color structure. Therefore, for the current purpose, it is sufficient to only present the associated gluon pole and color structure for each diagram.

We start the calculation by showing that the gauge link only receives contributions from the soft gluon pole in terms of momentum carried by the A^- gluon. All hard gluon pole contributions are canceled out. An explicit example is demonstrated in Figs. 4(a) and 4(b). When we

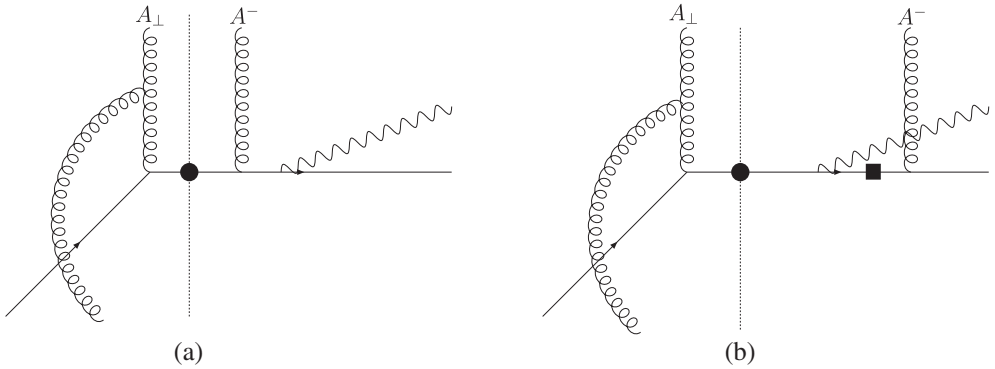

FIG. 4. The hard gluon pole is yielded when quark lines marked with a black circle go on shell, while the quark propagator marked with a black square gives rise to the soft gluon pole. Hard gluon pole contributions from (a) and (b) are canceled out due to the Ward identity.

isolate a hard gluon pole from the quark propagator marked with a black circle, the quark line is effectively put on shell. One then can apply the Ward identity argument to the part of the diagrams on the right side of the vertical dashed line. It is easy to verify that the hard gluon pole contributions are canceled out between Figs. 4(a) and 4(b) due to the Ward identity. One is only left with the soft gluon pole contribution generated from the quark propagator marked with black square in Fig. 4(b). Therefore, we only need to take into account the soft gluon pole of the A^- gluon from the initial-state interaction and final-state interaction. The relevant diagrams are shown in Fig. 6.

To simplify the calculation of diagrams with the three gluon vertex illustrated in Fig. 5, it is convenient to organize the A^+ and A^- gluon fusion amplitude into two terms,

$$\begin{aligned}&\frac{-igf^{abc}}{(x_gP+x_g'\bar{P})^2+i\epsilon}[g^{\mu\nu}(x_g'\bar{P}-x_gP)^\rho+g^{\nu\rho}(2x_gP+x_g'\bar{P})^\mu\\&\quad+g^{\rho\mu}(-2x_g'\bar{P}-x_gP)^\nu]n^\mu p^\nu\\&=\frac{-igf^{abc}(x_gP+x_g'\bar{P})^\rho}{(x_gP+x_g'\bar{P})^2+i\epsilon}-\frac{-igf^{abc}\bar{P}^\rho}{x_gP\cdot\bar{P}+i\epsilon},\end{aligned}\tag{18}$$

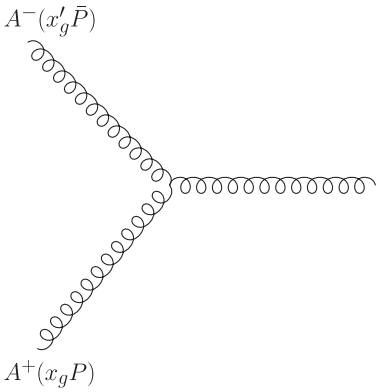

FIG. 5. Two longitudinally polarized gluons fusion diagram.

where the first term in the second line does not contribute to the final result due to the Ward identity. For example, the contribution from the first term is canceled out when summing up diagrams in Figs. 6(a), 6(d), and 6(i). One can use the second term as the effective Feynman rule for the A^+ and A^- gluon fusion vertex in the following calculation. It is important to notice that the associated gluon pole $\frac{1}{x_gP\cdot\bar{P}+i\epsilon}$ corresponds to the initial-state interaction contribution.

Using the above trick, it is easy to verify that the summation of the hard parts in Figs. 6(i), 6(j), and 6(k) vanishes,

$$\mathcal{H}_i+\mathcal{H}_j+\mathcal{H}_k=0.\tag{19}$$

And in an exactly analogous fashion, one has

$$\mathcal{H}_t+\mathcal{H}_u+\mathcal{H}_v=0.\tag{20}$$

Meanwhile, we also notice that

$$\mathcal{H}_h=0,\qquad \mathcal{H}_s=0.\tag{21}$$

We continue with the evaluation of Figs. 6(a) and 6(b),

$$\mathcal{H}_a\propto\frac{1}{x_g+i\epsilon}\frac{1}{-x_{g1}'-i\epsilon}\frac{1}{x_g'+i\epsilon}\mathrm{Tr}[T^aT^bT^cT^fT^e]if^{def}\tag{22}$$

$$\mathcal{H}_b\propto\frac{1}{x_g+i\epsilon}\frac{1}{-x_{g1}'-i\epsilon}\frac{1}{x_g'+i\epsilon}\mathrm{Tr}[T^aT^bT^fT^dT^e]if^{cef}.\tag{23}$$

Summing them up, one obtains

$$\begin{aligned}\mathcal{H}_{a+b}\propto&\frac{1}{x_g+i\epsilon}\frac{1}{-x_{g1}'-i\epsilon}\frac{1}{x_g'+i\epsilon}\\&\times\{C_F\mathrm{Tr}[T^aT^bT^cT^d]-\mathrm{Tr}[T^aT^bT^eT^cT^dT^e]\},\end{aligned}\tag{24}$$

which leads to the following gauge link structure:

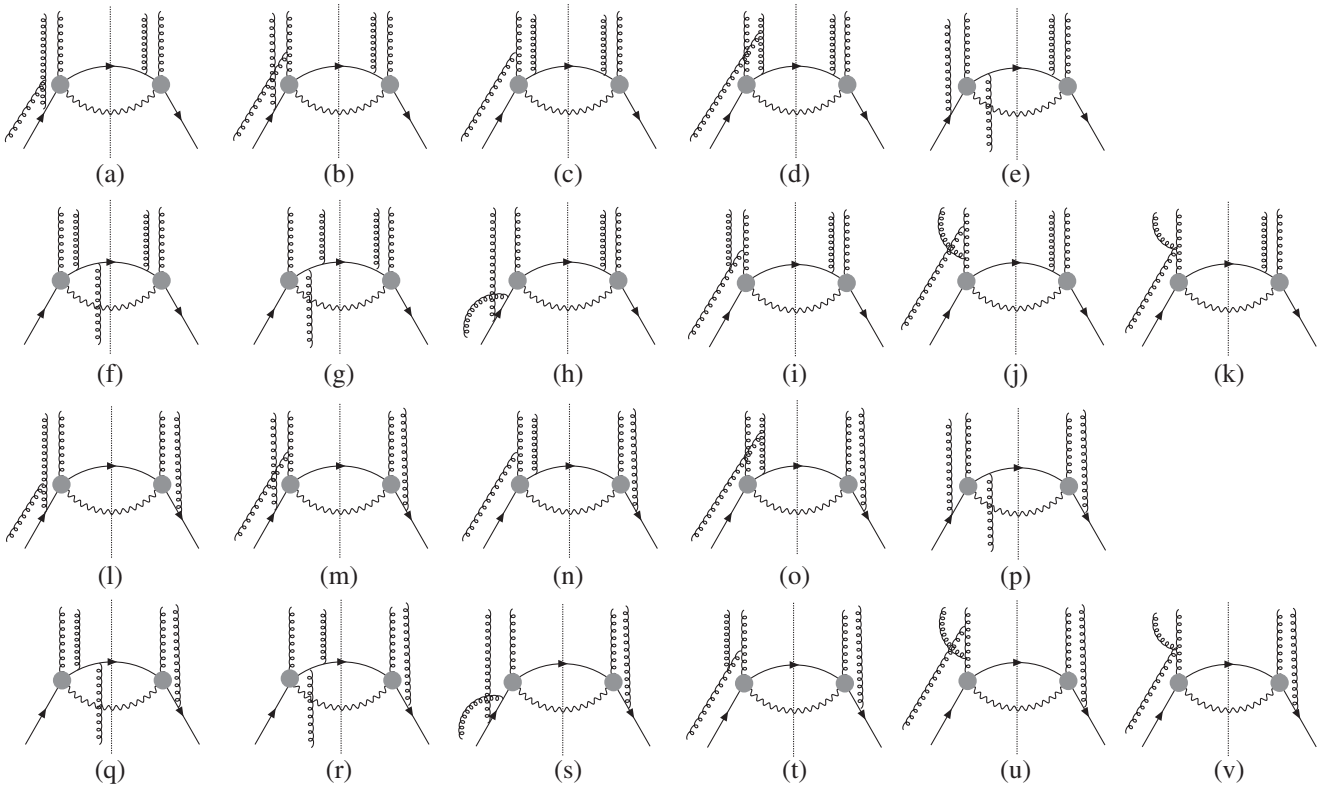

FIG. 6. The lowest nontrivial order diagrams giving rise to the color entanglement like effect. The mirror diagrams are not shown here. Gluons directly attaching to gray circles are transversely polarized. Other gluons from the top part of the diagrams are longitudinally polarized A^-, while the A^+ gluon is exchanged between hard parts and the bottom part. The contributions from (h,s) and the sum of (i,j,k,t,u,v) to the gauge link vanish if one uses the trick introduced after Eq. 18. The rest diagrams give rise to the nonvanishing contribution to the gauge link.

$$\mathcal{H}_{a+b} \Rightarrow C_F\langle P|\mathrm{Tr}\left[F_a^{-\mu}(\xi^+)T^a\left(ig\int_{\xi^+}^{\infty}dz^+T^bA_b^-(z)\right)F_c^{-\mu}(0)T^c\left(-ig\int_{-\infty}^{0}dz^+T^dA_d^-(z)\right)\right]|P\rangle$$
$$-\langle P|\mathrm{Tr}\left[F_a^{-\mu}(\xi^+)T^a\left(ig\int_{\xi^+}^{\infty}dz^+T^bA_b^-(z)\right)T^eF_c^{-\mu}(0)T^c\left(-ig\int_{-\infty}^{0}dz^+T^dA_d^-(z)\right)T^e\right]|P\rangle. \tag{25}$$

The gluon poles and color structures associated with Figs. 6(c) to 6(g) are listed in the following:

$$\mathcal{H}_c \propto \frac{1}{x_g+i\epsilon}\frac{1}{-x'_{g1}-i\epsilon}\frac{1}{-x'_g+i\epsilon}\mathrm{Tr}[T^aT^bT^dT^fT^e]if^{cef} \tag{26}$$

$$\mathcal{H}_d \propto \frac{1}{x_g+i\epsilon}\frac{1}{-x'_{g1}-i\epsilon}\frac{2l_q\cdot\bar{P}}{(l_q-x'_g\bar{P}-x_gP)^2+i\epsilon}\mathrm{Tr}[T^aT^bT^fT^cT^e]if^{def} \tag{27}$$

$$\mathcal{H}_e \propto \frac{-1}{-x_g+i\epsilon}\frac{1}{-x'_{g1}-i\epsilon}\frac{1}{x'_g+i\epsilon}\mathrm{Tr}[T^aT^bT^eT^cT^dT^e] \tag{28}$$

$$\mathcal{H}_f \propto \frac{-1}{-x_g+i\epsilon}\frac{1}{-x'_{g1}-i\epsilon}\frac{2l_q\cdot\bar{P}}{(l_q-x'_g\bar{P}-x_gP)^2+i\epsilon}\mathrm{Tr}[T^aT^bT^eT^dT^cT^e] \tag{29}$$

$$\mathcal{H}_g \propto \frac{-1}{-x'_g+i\epsilon}\frac{1}{-x'_{g1}-i\epsilon}\frac{2l_q\cdot P}{(l_q-x'_g\bar{P}-x_gP)^2+i\epsilon}\mathrm{Tr}[T^aT^bT^dT^eT^cT^e]. \tag{30}$$

We further decompose the hard parts $\mathcal{H}_d$ and $\mathcal{H}_f$ into two terms $\mathcal{H}_d=\mathcal{H}_{d1}+\mathcal{H}_{d2}$ and $\mathcal{H}_f=\mathcal{H}_{f1}+\mathcal{H}_{f2}$, where $\mathcal{H}_{d1}$, $\mathcal{H}_{f1}$ denote contributions by picking up the gluon poles, $\frac{1}{x_g+i\epsilon}$ and $\frac{1}{-x_g+i\epsilon}$, while the imaginary phase of $\mathcal{H}_{d2}$, $\mathcal{H}_{f2}$ is only

generated from the gluon pole $\frac{1}{(l_q-x'_gP-x_gP)^2+i\epsilon}$. When we isolate the imaginary phase from the pole $\frac{1}{(l_q-x'_gP-x_gP)^2+i\epsilon}$, an internal quark propagator is effectively put on shell. The Ward identity then implies that

$$\mathcal{H}_{d2}+\mathcal{H}_{f2}+\mathcal{H}_g=0. \tag{31}$$

This relation also can be readily verified by explicit calculation. The hard parts $\mathcal{H}_{f1}$ and $\mathcal{H}_e$ represent the final-state interaction contributions, which are canceled out by the corresponding left cut diagrams, as explained in the previous section. We are now only left with

$$\mathcal{H}_{c+d1}\propto\frac{1}{x_g+i\epsilon}\frac{1}{-x'_{g1}-i\epsilon}\frac{1}{-x'_g+i\epsilon}\{C_F\mathrm{Tr}[T^aT^bT^dT^c]-\mathrm{Tr}[T^aT^bT^eT^dT^cT^e]\}, \tag{32}$$

which results in

$$\begin{aligned}\mathcal{H}_{c+d1}\Rightarrow\ & C_F\langle P|\mathrm{Tr}\left[F_a^{-\mu}(\xi^+)T^a\left(ig\int_{\xi^+}^{\infty}dz^+T^bA_b^-(z)\right)\left(-ig\int_0^{\infty}dz^+T^dA_d^-(z)\right)F_c^{-\mu}(0)T^c\right]|P\rangle\\ &-\langle P|\mathrm{Tr}\left[F_a^{-\mu}(\xi^+)T^a\left(ig\int_{\xi^+}^{\infty}dz^+T^bA_b^-(z)\right)T^e\left(-ig\int_0^{\infty}dz^+T^dA_d^-(z)\right)F_c^{-\mu}(0)T^cT^e\right]|P\rangle.\end{aligned} \tag{33}$$

A similar analysis applies to the rest of diagrams. One finds that

$$\mathcal{H}_{o2}+\mathcal{H}_{q2}+\mathcal{H}_r=0 \tag{34}$$

and the contributions from $\mathcal{H}_{q1}$ and $\mathcal{H}_p$ drop out once combined with the corresponding left cut diagrams. One eventually has

$$\begin{aligned}\mathcal{H}_{l+m}\Rightarrow\ & C_F\langle P|\mathrm{Tr}\left[\left(ig\int_{-\infty}^{\xi^+}dz^+T^bA_b^-(z)\right)F_a^{-\mu}(\xi^+)T^aF_c^{-\mu}(0)T^c\left(-ig\int_{-\infty}^{0}dz^+T^dA_d^-(z)\right)\right]|P\rangle\\ &-\langle P|\mathrm{Tr}\left[\left(ig\int_{-\infty}^{\xi^+}dz^+T^bA_b^-(z)\right)F_a^{-\mu}(\xi^+)T^aT^eF_c^{-\mu}(0)T^c\left(-ig\int_{-\infty}^{0}dz^+T^dA_d^-(z)\right)T^e\right]|P\rangle\end{aligned} \tag{35}$$

and

$$\begin{aligned}\mathcal{H}_{n+o1}\Rightarrow\ & C_F\langle P|\mathrm{Tr}\left[\left(ig\int_{-\infty}^{\xi^+}dz^+T^bA_b^-(z)\right)F_a^{-\mu}(\xi^+)T^a\left(-ig\int_0^{\infty}dz^+T^dA_d^-(z)\right)F_c^{-\mu}(0)T^c\right]|P\rangle\\ &-\langle P|\mathrm{Tr}\left[\left(ig\int_{-\infty}^{\xi^+}dz^+T^bA_b^-(z)\right)F_a^{-\mu}(\xi^+)T^aT^e\left(-ig\int_0^{\infty}dz^+T^dA_d^-(z)\right)F_c^{-\mu}(0)T^cT^e\right]|P\rangle.\end{aligned} \tag{36}$$

Collecting all pieces $\mathcal{H}_{a+b},\mathcal{H}_{c+d1},\mathcal{H}_{l+m},\mathcal{H}_{n+o1}$ together, it is easy to see that the summation of them gives rise to the lowest nontrivial order expansion of the gauge link structure

$$\begin{aligned}&C_F\langle P|\mathrm{Tr}[F_a^{-\mu}(\xi^+)T^a\mathcal{L}(\xi^+,0)F_c^{-\mu}(0)T^c\mathcal{L}^\dagger(\xi^+,0)]|P\rangle\\ &-\langle P|\mathrm{Tr}[\mathcal{L}^\dagger(-\infty,\xi^+)F_a^{-\mu}(\xi^+)T^a\mathcal{L}^\dagger(\xi^+,\infty)T^e\mathcal{L}(\infty,0)F_c^{-\mu}(0)T^c\mathcal{L}(0,-\infty)T^e]|P\rangle,\end{aligned} \tag{37}$$

where the term in the second line has quite a peculiar color structure. Note that the final-state interactions $\mathcal{H}_{q1},\mathcal{H}_p,\mathcal{H}_{f1}$, and $\mathcal{H}_e$ contribute to the twist-2 unpolarized cross section. The principal value part of the gluon poles $\frac{1}{-x_g+i\epsilon}$ and $\frac{1}{x_g+i\epsilon}$ is canceled out when adding up these contributions with the second term in the above formula. Correspondingly, A^+ gluon attachment is decoupled from the hard part and can be absorbed into the gauge link of the collinear quark distribution. This leads us to conclude that the collinear twist-2 factorization is not affected by the color entanglement–like effect at the order under consideration. Meanwhile, it becomes clear that the emergence of

the color entanglement–like effect in the collinear twist-3 factorization essentially can be attributed to the fact that the final-state interaction does not contribute to the SSA. With this observation, one can generalize the above analysis to all orders. Considering a diagram with an arbitrary number of A^- gluon attachments and one A^+ attachment from the opposite side, the A^+ gluon can be first decoupled from the hard part by invoking the Ward identity argument once we sum over all possible A^+ insertion points. After this has been done, multiple A^- exchange can be incorporated into the normal gauge link as shown in the first line of Eq. (37). However, one has to keep in mind that only initial -state interaction contributes to the SSA in the current case. The gauge link structure associated with final-state interaction given in the second line of Eq. (37) has to be subtracted. The overall color structure associated with initial-state interaction is thus given by Eq. (37). Note that a similar argument also applies to the SSA in other channels, for instance, inclusive hadron production in pp collisions, because initial-state interaction and final-state interaction do not generate contributions with equal weight.

Equation (37) can be further cast into the following form using the Fierz identity:

$$\frac{N_c}{2}\langle P|\mathrm{Tr}[F_a^{-\mu}(\xi^+)T^a\mathcal{L}(\xi^+,0)F_c^{-\mu}(0)T^c\mathcal{L}^\dagger(\xi^+,0)]|P\rangle - \frac{1}{2}\langle P|\mathrm{Tr}[\mathcal{L}^\dagger(-\infty,\xi^+)F_a^{-\mu}(\xi^+)T^a\mathcal{L}^\dagger(\xi^+,\infty)]\mathrm{Tr}[\mathcal{L}(\infty,0)F_c^{-\mu}(0)T^c\mathcal{L}(0,-\infty)]|P\rangle. \tag{38}$$

One immediately recognizes this operator structure as the one that gives rise to the combination $x'G(x') - x'G_4(x')$. The corresponding spin-dependent cross section reads

$$\frac{d^3\Delta\sigma}{d^2l_{\gamma\perp}dz} = \frac{\alpha_s\alpha_{em}N_c}{N_c^2-1}\frac{(z^2-z)[1+(1-z)^2]}{l_{\gamma\perp}^4}\frac{\epsilon^{l_\gamma S_\perp np}}{l_{\gamma\perp}^2}\sum_q e_q^2\int_{x_{\min}}^1 dx[x'G(x') - x'G_4(x')]\left[-x\frac{d}{dx}T_{F,q}(x,x)\right], \tag{39}$$

which is in full agreement with that obtained by extrapolating the hybrid approach result to the collinear limit [13]. As expected, the pure collinear twist-3 formalism and the hybrid approach are consistent with each other in the collinear limit after properly taking into account the color entanglement–like effect in the collinear twist-3 formalism.

It is worth it to mention that there is a substantial difference between the color entanglement like effect in TMD factorization and the color entanglement–like effect in collinear factorization. In the current case, a nontrivial color structure characterized by a G_4 term yielded by taking into account longitudinal gluon attachments from both incoming nucleons does not lead to the breakdown of collinear twist-3 factorization at the order under consideration. It is still possible to describe physical observables in terms of the correlators associated with each nucleon separately. As a consequence, the predicative power is preserved in collinear twist-3 factorization.

We finish this section with a final remark. In this work, we focus on the $qg \to \gamma q$ channel as it is the dominant source contributing to the SSA in the forward region. From the theoretical point of view, it is also interesting to study whether a nontrivial color structure shows up in the $q\bar{q} \to \gamma g$ channel. This is likely to be the case as the Ward identity argument fails due to the absence of the final-state interaction for the T-odd observable. However, it is not clear if the relevant contribution can be factorizable in a similar fashion or not. This deserves a further investigation in the future.

IV. SUMMARY

In summary, we have shown that the color entanglement–like effect plays a role in contributing to T-odd observables within the genuine collinear twist-3 factorization framework. For an example, we compute the SSA for direct photon production in pp collisions using the collinear twist-3 approach. Our calculation differs from the conventional collinear twist-3 treatment by deriving the gauge link structure on the unpolarized target side explicitly. We found that the existence of the longitudinal gluon A^+ attachment from the polarized projectile leads to a peculiar gauge link structure when summing up A^- gluon exchanges, which can be summarized into the novel gluon distribution G_4. As expected, the pure collinear twist-3 formalism and the hybrid approach do yield the same result in the overlap region where they both apply. We emphasize that this is the first instance of observable effects due to nontrivial gauge links in collinear factorization.

In the present work, we only focus on the derivative term contribution. But we anticipate that the nonderivative term contribution and the soft fermion pole contribution [22] are also affected by the color entanglement–like effect. Moreover, it has been found in the hybrid approach calculations [17–19] that the color entanglement–like effect

also contributes to the SSAs in other processes in pp/pA collisions. It is of great interest to confirm these results within the pure collinear twist-3 approach, particularly in view of the fact that the color entanglement–like effect plays a crucial role in solving the sign mismatch problem [19]. However, not all of the previous calculations for T-odd observables (for instance, the SSA for jet production in Semi-inclusive deeply inelastic scattering) are affected by the identified color entanglement–like effect. Nevertheless, many previous collinear twist-3 calculations for T-odd observables (including those related to the Boer-Mulders effect [23–26]) should be thoroughly reexamined by analyzing the gauge link structure of the collinear twist-2 parton distributions on the target side.

There are also some other theoretical issues that remain to be addressed in future study. First of all, one has to investigate if all pure gauge gluon A^+ attachments other than the one carrying small transverse momentum can be decoupled from hard parts and absorbed into the gauge link in the ETQS function. If true, relevant cross sections are factorizable in collinear twist-3 factorization. Otherwise, collinear twist-3 factorization breaks down for T-odd observables in pp collisions. Second, it is worth making an effort to study the properties of the gluon distribution G_4 at moderate or large x, such as its scale evolution and behavior in some models. Finally, though we tend to believe that the conventional collinear twist-3 formulation of T-even observables [27–31] and fragmentation effects [32–39] are not affected by the color entanglement–like effect, it would be nice to verify this point by explicit calculations.

ACKNOWLEDGMENTS

This work has been supported by the National Science Foundation of China under Grant No. 11675093 and by the Thousand Talents Plan for Young Professionals.

[1] J. C. Collins and D. E. Soper, Nucl. Phys. **B193**, 381 (1981); **B213**, 545(E) (1983); **B213**, 545 (1983); **B194**, 445 (1982).
[2] C. J. Bomhof, P. J. Mulders, and F. Pijlman, Phys. Lett. B **596**, 277 (2004).
[3] A. Bacchetta, C. J. Bomhof, P. J. Mulders, and F. Pijlman, Phys. Rev. D **72**, 034030 (2005).
[4] C. J. Bomhof, P. J. Mulders, and F. Pijlman, Eur. Phys. J. C **47**, 147 (2006).
[5] J. Collins and J. W. Qiu, Phys. Rev. D **75**, 114014 (2007).
[6] T. C. Rogers and P. J. Mulders, Phys. Rev. D **81**, 094006 (2010).
[7] M. G. A. Buffing and P. J. Mulders, J. High Energy Phys. 07 (2011) 065; Phys. Rev. Lett. **112**, 092002 (2014).
[8] M. G. A. Buffing, A. Mukherjee, and P. J. Mulders, Phys. Rev. D **86**, 074030 (2012).
[9] T. C. Rogers, Phys. Rev. D **88**, 014002 (2013).
[10] A. Adare *et al.* (PHENIX Collaboration), Phys. Rev. D **95**, 072002 (2017).
[11] J. Qiu and G. Sterman, Nucl. Phys. **B378**, 52 (1992);
[12] C. Kouvaris, J. W. Qiu, W. Vogelsang, and F. Yuan, Phys. Rev. D **74**, 114013 (2006).
[13] A. Schafer and J. Zhou, Phys. Rev. D **90**, 034016 (2014).
[14] P. J. Mulders and J. Rodrigues, Phys. Rev. D **63**, 094021 (2001).
[15] A. V. Efremov and O. V. Teryaev, Yad. Fiz. **36**, 242 (1982) [Sov. J. Nucl. Phys. **36**, 140 (1982)]; Phys. Lett. B **150**, 383 (1985).
[16] J. Qiu and G. Sterman, Phys. Rev. Lett. **67**, 2264 (1991).
[17] A. Schafer and J. Zhou, Phys. Rev. D **90**, 094012 (2014).
[18] J. Zhou, Phys. Rev. D **92**, 014034 (2015).
[19] J. Zhou, Phys. Rev. D **96**, 034027 (2017).
[20] X. Ji and F. Yuan, Phys. Lett. B **543**, 66 (2002).
[21] A. V. Belitsky, X. Ji, and F. Yuan, Nucl. Phys. **B656**, 165 (2003).
[22] K. Kanazawa and Y. Koike, Phys. Lett. B **720**, 161 (2013).
[23] D. Boer and P. J. Mulders, Phys. Rev. D **57**, 5780 (1998).
[24] J. Zhou, F. Yuan, and Z. T. Liang, Phys. Rev. D **78**, 114008 (2008).
[25] J. Zhou, F. Yuan, and Z. T. Liang, Phys. Lett. B **678**, 264 (2009).
[26] K. Kanazawa, Y. Koike, A. Metz, and D. Pitonyak, Phys. Rev. D **91**, 014013 (2015).
[27] J. Zhou, F. Yuan, and Z. T. Liang, Phys. Rev. D **81**, 054008 (2010).
[28] Z. T. Liang, A. Metz, D. Pitonyak, A. Schafer, Y. K. Song, and J. Zhou, Phys. Lett. B **712**, 235 (2012).
[29] A. Metz, D. Pitonyak, A. Schaefer, and J. Zhou, Phys. Rev. D **86**, 114020 (2012).
[30] Y. Hatta, K. Kanazawa, and S. Yoshida, Phys. Rev. D **88**, 014037 (2013).
[31] Y. Koike, D. Pitonyak, and S. Yoshida, Phys. Lett. B **759**, 75 (2016).
[32] F. Yuan and J. Zhou, Phys. Rev. Lett. **103**, 052001 (2009).
[33] Z. B. Kang, F. Yuan, and J. Zhou, Phys. Lett. B **691**, 243 (2010).
[34] J. Zhou and A. Metz, Phys. Rev. Lett. **106**, 172001 (2011).
[35] A. Metz and D. Pitonyak, Phys. Lett. B **723**, 365 (2013); **762**, 549(E) (2016).
[36] K. Kanazawa, Y. Koike, A. Metz, and D. Pitonyak, Phys. Rev. D **89**, 111501 (2014).
[37] Y. Hatta, B. W. Xiao, S. Yoshida, and F. Yuan, Phys. Rev. D **95**, 014008 (2017).
[38] L. Gamberg, Z. B. Kang, D. Pitonyak, and A. Prokudin, Phys. Lett. B **770**, 242 (2017).
[39] A. Metz and A. Vossen, Prog. Part. Nucl. Phys. **91**, 136 (2016).